Ozone trends from 2005 to 2016 at the Manitou Springs Station: attainment of the lowered ozone NAAQS in Colorado Springs

Presented to

The Faculty of the Environmental Program

Colorado College

In Partial Fulfillment of the Requirements for the Degree

Bachelor of Arts in Environmental Science

By

Yingxuan Li

May/2017

Thesis advisors:

Lynne Gratz

Signature: _____

Howard Drossman

Signature: _____

Table of Contents

Abstract

Hourly averaged ozone (O_3) measurements from 2005-2016 collected at the Manitou Springs station, Colorado, were analyzed to determine long-term trends and assess the ability for the Colorado Springs metropolitan area to be in attainment of the O_3 National Ambient Air Quality Standards (NAAQS). The EPA recently lowered the NAAQS for O_3 from 75 ppbv to 70 ppbv, posing attainment challenges for high elevation regions of the western United States, including Colorado Springs, due to the impacts of baseline O_3. Baseline O_3 is defined as O_3 that is transported to a location from upwind sources. This study aims to identify possible causes of different O_3 trends in Colorado Springs. The annual 99th percentile O3 concentration showed a significant decrease of -0.71 ppbv yr^{-1} (-0.96% ppbv yr^{-1}), and the annual 5th percentile significantly increased by 0.81 ppbv yr^{-1} (5.8% ppbv yr^{-1}), while the annual 50th and 95th percentiles did not show significant trends. The decreasing trends generally appeared to occur at the 95th and 99th percentiles, attributing to the effectiveness of both local and nationwide O_3 precursor emission controls. The increasing trend in the 5th percentile indicates possible increased baseline ozone. Seasonal variability of O_3 concentrations was present with 50th percentile O_3 values in spring (45 ppbv) and summer (46 ppbv) being significantly higher than fall (36 ppbv) and winter (35 ppbv), in part due to the seasonal patterns of photolysis conditions and temperature. Although multiple studies have observed increasing trends in springtime O_3 in the western U.S., no such spring trends were observed this analysis. The lack of significant trends may be due to the particular location and topography of the monitoring site, which is east of the Continental Divide and in the foothills of the Pikes Peak region, as well as the influence from the nearby urban emissions. We also

performed cluster analysis of 10-day HYSPLIT back-trajectories generated for spring (April-May) and summer (June-August) and looked at O_3 trends within each cluster. For spring, most of the clusters did not indicate significant linear trends; the only significant positive trend was associated with low-altitude transport over the Pacific (Cluster 2). For summer, a significant positive trend was found in the 95th percentile of Cluster 6, representing the low-altitude transport from the southeast. The wintertime 5th and 50th percentiles indicated significant increases, with slopes of 1.13 ppbv yr^{-1} (17.2% ppbv yr^{-1}) and 0.3 ppbv yr^{-1} (0.93% ppbv yr^{-1}). Rapid development of oil and natural gas industry around the area may contribute to these positive trends, and this is an area for future research.

1. Introduction

Under the Clean Air Act, the US Environmental Protection Agency (EPA) has a statutory duty to periodically review the National Ambient Air Quality Standards (NAAQS) for six criteria pollutants, including particulate matter (PM), sulfur dioxide (SO_2), nitrogen oxides (NO_x = NO + NO_2), carbon monoxide (CO), lead (Pb), and ozone (O_3) (EPA, 2017). The reviews are to be based on scientific evidence and analysis, and they are designed to ensure that air quality standards are adequately protecting the public health and welfare (EPA, 2015).

Since 1980, air quality has improved nationally based on concentrations of the criteria pollutants, attributing to the effectiveness of regulatory and pollution-control programs, such as State Implementation Plans (EPA, 2017). Particularly in the eastern US, pollutant trends have been shown to decrease for many criteria pollutants including PM, NO_x, SO_2, and CO (Austin et al., 2015; Parrish et al., 2011, EPA, 2017). However,

trends for O_3 have a more mixed result. The maximum daily 8-hour averaged surface O_3 showed a national decrease of 17% over 2000 to 2015 (EPA, 2017). The domestic anthropogenic emissions of O_3 precursors, including NO_x, CO and volatile organic compounds (VOCs), declined from 2000 to 2015 by 49%, 50%, and 19%, respectively (EPA, 2017). In particular, reductions in NO_x emissions between 2005 and 2011 were evident in satellite observations of NO_2 concentrations across the U.S. (Fig 1; NASA, 2014). One might expect that this should have resulted in decreases in O_3 concentrations across the country. However, in the western U.S. although decreases in summertime O_3 were observed, multiple studies have found significant positive trends in spring and winter time O_3 in the free troposphere and at the high elevation rural sites, even though domestic O_3 precursor emissions have substantially reduced (Cooper et al.; 2012; Simon et al., 2015; Lin et al.; 2017). A number of researchers relate this phenomenon with trans-Pacific transport of O_3 and O_3 precursors from Asia and intrusions from the upper troposphere/lower stratosphere (UT/LS) (Gratz et al., 2014; Lin et al.; 2017; Baylon et al., 2016). Thus from a regulatory perspective, a better understanding of the factors driving long-term changes in O_3 concentration is crucial for making air quality standard and for designing appropriate control policies.

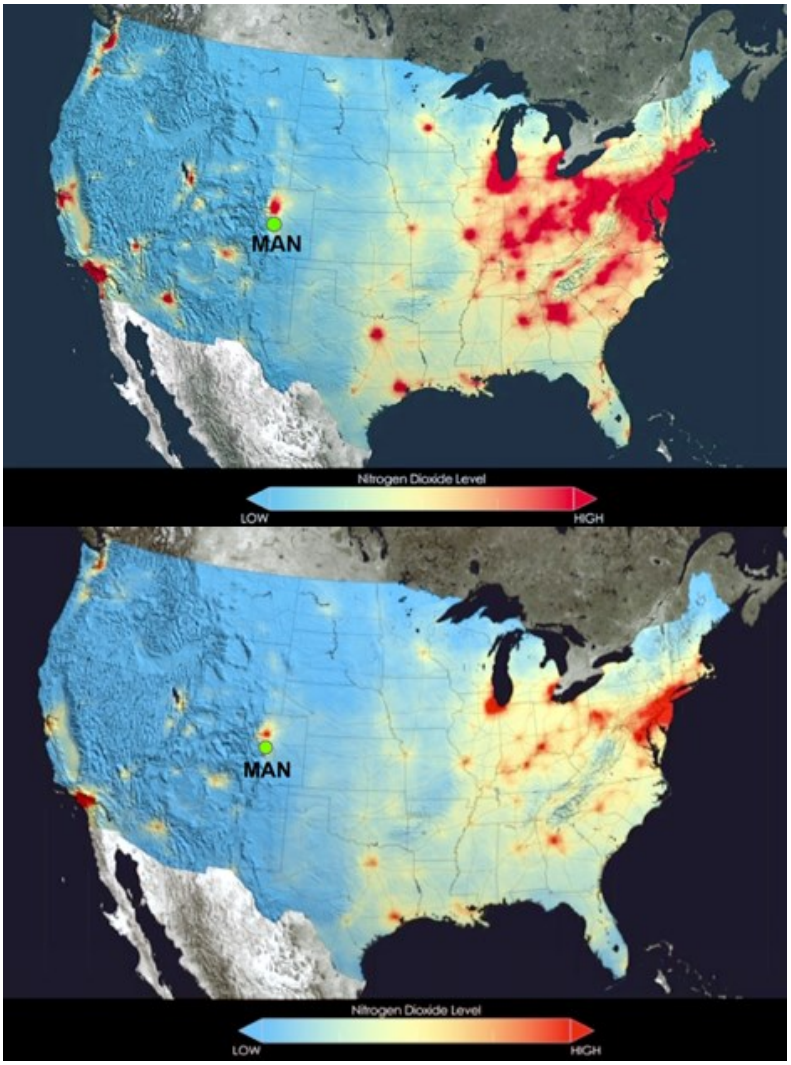

Figure 1 Tropospheric column concentrations of NO_2 across the U.S. as detected by the Ozone Monitoring Instrument on NASA's Aura satellite. The figure above is based on measurements from 2005, and the figure below is based on measurements from 2011 (NASA, 2014). The location of the Manitou Spring monitoring station, the focus of this work, is also noted on the maps.

Ozone is a gas that exists in both the Earth's stratosphere and troposphere. Tropospheric O_3 is the precursor of the hydroxyl radical (OH) and plays a key role in controlling the oxidizing capacity of the troposphere (Baylon et al., 2016). It is also of environmental importance as a greenhouse gas and as a toxic pollutant to humans and vegetation in surface air, because it oxidizes biological tissue (Jacob, 1999). In contrast to the "good" O_3 in the stratosphere that forms a protective layer to shield life on earth from

the harmful solar ultraviolet rays, ground level O_3 has direct adverse impacts on human and environmental health. Ground level O_3 is a major component of urban smog, and breathing it can trigger a variety of health problems including chest pain, coughing, throat irritation, airway inflammation, and upper and lower respiratory diseases such as asthma, bronchitis, heart attack, and other cardiovascular problems (Weinhold, 2008). Elevated O_3 concentrations in surface air may also cause negative impacts on agricultural and forest yields, sensitive vegetation, and natural ecosystems (EPA, 2017). Rather than being directly emitted like many other pollutants, tropospheric O_3 is either transported from the stratosphere to the troposphere, or at ground level predominantly formed as a secondary pollutant from photochemical reactions involving NO_x and VOCs from both mobile and stationary sources (Jacob, 1999; EPA, 2017). The term VOCs encompasses all organics, such as hydrocarbons, aldehydes, alcohols, nitrogen and sulfur-containing organics, etc. (Finlayson-Pitts & Pitts Jr, 1993).

Ozone is formed in the troposphere from the oxidation of VOCs and CO by OH in the presence of NO_x and sunlight (Jacob, 1999); the chemical reactions of O_3 formation are shown below, where RO_2 represents any of a number of organic molecules with an O-O bond attached (Sillman, 2003; Jacob, 1999). In densely populated regions with high emissions of NO_x and VOCs, rapid O_3 production can take place and result in surface air pollution (Jacob, 1999). NO_x and VOCs are typically emitted from sources such as industrial facilities and electric utilities, motor vehicle exhaust, gasoline vapors, and chemical solvents (Weinhold, 2008). Substantial O_3 formation in the troposphere requires both NOx and VOC precursors, and control of O_3 is generally achieved by reducing the anthropogenic emissions of NOx and VOCs into the atmosphere (Weinhold, 2008).

Moreover, NO_x molecules also participate in O_3 destruction reactions (R7). In the vicinity of large NO emissions (e.g. power plants), O_3 concentrations are depressed through the process of NO_x titration resulting in net conversion of O_3 to NO_2 (Sillman, 2003).

$$VOC + OH \overset{O_2}{\rightarrow} RO_2 + H_2O \quad \text{R1}$$

$$CO + OH \overset{O_2}{\rightarrow} HO_2 + CO_2 \quad \text{R2}$$

$$RO_2 + NO \overset{O_2}{\rightarrow} secondary\ VOC + HO_2 + NO_2 \quad \text{R3}$$

$$HO_2 + NO \rightarrow OH + NO_2 \quad \text{R4}$$

$$NO_2 + hv \rightarrow NO + O \quad \text{R5}$$

$$O + O_2 + M \rightarrow O_3 + M \quad \text{R6}$$

$$NO + O_3 \rightarrow NO_2 + O_2 \quad \text{R7}$$

Long-range transport of O_3 and O_3 precursors also importantly contributes to O_3 concentrations at regional and local scales in the U.S. (Zhang et al., 2008). Several studies report that transport of precursor emissions from as far away as Asia can impact the air quality in western US (Lin et al., 2017; Parrish et al., 2012). Mid-latitude cyclones are considered to be the main mechanism for lifting Asian pollutions into the free troposphere over the western Pacific, and once the pollution is over the western Pacific, it can then be rapidly transported by strong westerly winds (Liang et al., 2005). The major pathways for trans-Pacific transport are the warm conveyor belts (WCBs), where polluted air is lifted into the WCBs and then rapidly transported in the middle and upper troposphere over long distances (Parrish et al., 2012). Many studies indicate that long-range transport of O_3 is most pronounced in spring, when Asian outflow to the Pacific is particularly strong due to the low-pressure systems in northeastern Asian and strong westerly winds over the high emission regions (Zhang et al., 2008; Liang et al., 2005).

Transport from the UT/LS or stratospheric intrusions may also contribute to the high tropospheric O_3 events over high-altitude locations in the western U.S. (Lin et al., 2015). Intrusions of stratospheric air into the troposphere occur when cold, dry and O_3-rich air descends from the stratosphere toward the surface, and over the mountainous western U.S.intrusions can reach the surface because of the high elevation (Sullivan et al., 2015). Concentrations of tropospheric O_3 are therefore affected by many factors, making it difficult to predict O_3 concentrations based solely on the local sources of emission. Thus, understanding global and regional sources of local air pollution is crucial for setting air quality standards and for designing appropriate control policies.

On October 1, 2015, based on the review of the air quality criteria for O_3 and related photochemical oxidants and for O_3 production (EPA, 2017), the EPA revised the primary and secondary ground-level O_3 standard levels from 0.075 parts per million (ppm) to 0.070 ppm. The design values are calculated based on the three-year average of the "fourth-highest daily maximum over an eight-hour period of measurements" (EPA, 2017). The establishment of the new O_3 standard reflected the results of the standard review processes and was based on extensive scientific analysis to ensure the standards are adequate to protect public health and welfare (EPA, 2017). However, this lowered standard may pose O_3 attainment challenges for high elevation regions of the western U.S., including Colorado Springs, due to contributions of baseline O_3 and stratospheric intrusions to ground level O_3 mixing ratios (Simon et al., 2014; Sullivan et al., 2015).

Baseline O_3 refers to O_3 that is produced when local emission influences are determined to be negligible. Baseline sources of O_3 are associated with both natural processes, like stratospheric intrusions and wildfire, and trans-Pacific transport of O_3

(Cooper et al., 2012). Increasing levels of baseline O_3 may offset some of the O_3 reductions efforts from local O_3 precursor emissions reductions, suggesting that new approaches to dealing with O_3 control policies and with attainment status may be necessary. Traditional control strategies for O_3 focus on reducing local anthropogenic emission sources, but regulatory justifications of "exceptional events" and baseline O_3 due to natural or uncontrollable causes may also need to be addressed, so that an area would not be designated as non-attainment for sources that exceed its jurisdiction.

This study explores annual and seasonal O_3 trends from 2005 to 2016 at the air quality monitoring station in Manitou Springs, Colorado, U.S.A. Cluster analysis of 10-day back-trajectories from the Manitou Springs station was also performed using HYSPLIT version 4 for spring and summer months, and O_3 trends were examined within each cluster. Most of the analysis was focused on spring and summer, because these are the seasons that are most likely to exceed the lowered NAAQS for O_3. Fall and winter O_3 trends were also calculated to contrast O_3 trends between seasons. Combining O_3 measurements with the trajectory analysis, this study aims to identify possible causes of different O_3 trends at the Manitou Springs station and provide a baseline for future research into the significance of long-range transport of O_3 in Colorado Springs.

2. Methods

2.1 Measurement site description

The city of Colorado Springs is located in El Paso County in the Pikes Peak region of Colorado. The city is on average 1839 m above sea level and is located on the eastern side of the Southern Rocky Mountains, approximately 105 km south of the State Capital of Denver (CDT, 2017; Fig. 2). With a land area of approximately 505 km^2 and

an estimated population of 457,000 as of the 2015 Census, Colorado Springs is the largest city in terms of area, and the second most populous city in Colorado (USCB, 2015; CDT, 2017). Vehicle usage, coal-fired power plants, and oil and gas drilling are large contributors to ground-level O_3 in the area (CDPHE, 2016).

Manitou Springs is located 6 km west of Colorado Springs (Fig. 2). The Manitou Springs monitoring station for the Colorado Department of Public Health and Environment (CDPHE) (38.853097º N, 104.901286º W, 1955 m above sea level) is located in the foothills above Colorado Springs behind the city maintenance facility (CDPHE, 2015). It is classified as a "population-oriented neighborhood scale" State or Local Air Monitoring Stations (SLAMS) monitor. Ozone monitoring began in April 2004, and hourly-averaged O_3 measurements have been collected continuously since that time. Ozone is currently measured using a Teledyne model T400 ozone analyzer at the Manitou Springs station. Prior observations and modeling in the Colorado Springs area indicate that high O_3 concentrations usually spread along the Monument Creek drainage to the north of the Colorado Springs central business district (CBD), or to a lesser extent along the Fountain Creek drainage to the west of the CBD (CDPHE, 2015). A second O3 monitoring station for Colorado Springs is located at the United States Air Force Academy (USAFA). This monitoring station is near the Monument Creek drainage, approximately 15 km north of the Colorado Springs CBD to capture the high O_3 concentrations (Fig. 2). Ozone monitoring at the USAFA started in May 1996, and the site is near the south entrance of the Academy but away from the highway I-25 (CDPHE, 2015). The Manitou Springs station was established because of the concerns that high concentrations of urban O_3 might travel farther up the Fountain Creek drainage and the

USAF Academy monitoring station was not sufficient to detect all the high O_3 concentrations (CDPHE, 2015). The Manitou Springs station was chosen for this study because it is relatively closer to the Colorado Springs CBD, and O_3 observations at this site represent influence from both baseline conditions and fresh local pollution.

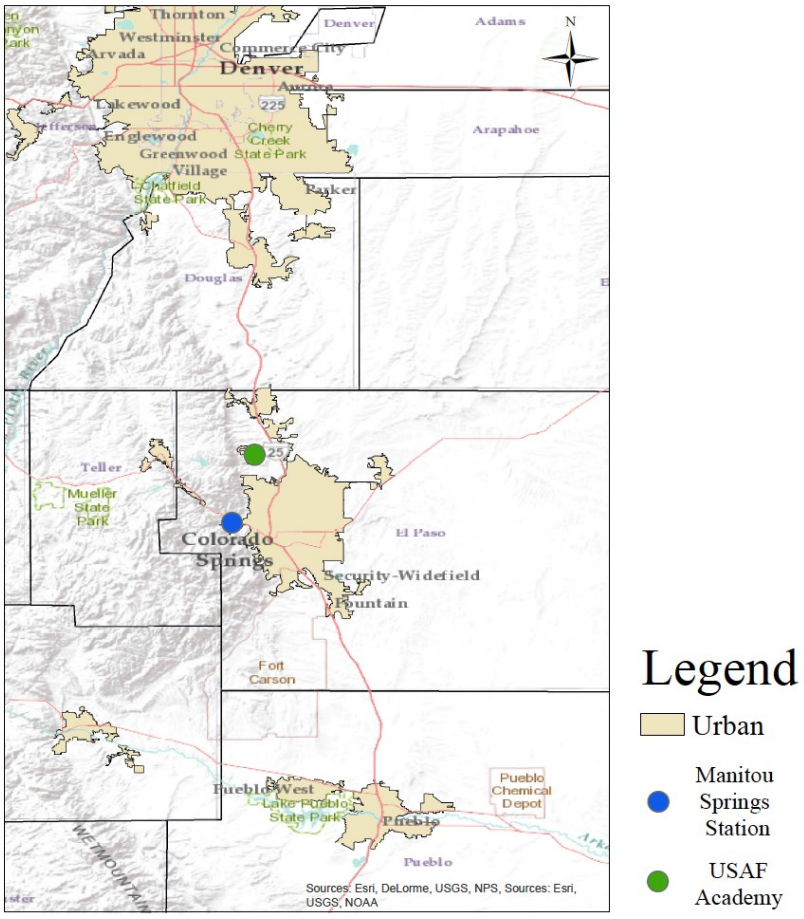

Figure 2 Topographic map of Colorado Springs and Denver areas including the locations of the Manitou Springs and the USAF Academy stations.

2.2 Data Analysis

Hourly-averaged O_3 measurements from 2005 to 2015 were used in annual, seasonal, and cluster trend analysis. In all cases, trends were calculated separately for the annual 5^{th}, 50^{th}, 95^{th}, and 99^{th} percentile of the hourly O_3 data. The percentiles for each

year were calculated from all hourly O_3 values for the year. I used linear regression with a one-way ANOVA to determine the trends. I also used one-way ANOVA and Independent-samples t-test to compare the differences between clusters and seasons. The slopes of the linear regression indicate the rate of change in O_3 mixing ratio per year for 2005-2015 in ppbv yr^{-1}, and they are reported with 95% confidence intervals. The p-value indicates the statistical significance of the linear relationship, and trends are referred to as statistically significant for $p<0.05$. Annual percent changes in O_3 were calculated by dividing the slope by the intercept. I carried out the data analysis using SPSS version 21 and Microsoft Excel.

2.3 HYSPLIT back-trajectory cluster analysis

Ten-day air mass back-trajectories from the Manitou Springs station were computed for every fourth hour in April-August 2005-2015 using the Hybrid Single-Particle Lagrangian Integrated Trajectory model (HYSPLIT) version 4 (Draxler & Hess, 1998). Gridded meteorological data was obtained from the National Oceanographic and Atmospheric Administration Air Resources Laboratory (NOAA-ARL) (Draxler & Hess, 1998). HYSPLIT has been widely used for computing air mass trajectory and dispersion simulations (Draxler & Hess, 1998). It plots the position of an individual air parcel through time as it is transported by three-dimensional winds (Stein et al., 2016). One of the most common model applications is the back-trajectory analysis to determine the origin of air masses and establish source-receptor relationships (Fleming, 2011). Trajectory calculations are achieved by the time integration of the position of the air parcel as it follows the average meteorological patterns (Stein et al., 2016). Moreover, HYSPLIT is a probability model, with each data point relying on the probability of the

previous one. Thus, due to assumptions in the wind fields used to calculate the trajectories, the uncertainty of trajectories increases with distance from the starting location (Fleming et al., 2012).

For 2005-2015, the Global Data Assimilation System (GDAS) $1^o \times 1^o$ gridded meteorology data with a starting height of 500m above ground level was used. The model was configured to compute backward trajectories starting daily at 0:00 MDT, with each trajectory having a duration of 10 days totaling 240 hours. Ozone and its precursors can be transported thousands of kilometers from the source within 10 days, and therefore trajectories of this length allow for identifying potential long-range O_3 transport pathways. The lifetime of O_3 in the free troposphere can be on the order of several weeks depending on season and altitude, and the trans-Pacific transport of O_3 pollution from Asia across the Pacific can occur in 5 to 10 days (Zhang et al, 2008). Thus the duration of 10 days was chosen in this study to detect the potential trans-Pacific transport of O_3 pollution in Colorado Springs. For spring, multiple studies observed that the trans-Pacific transport of O_3 pollution has the greatest impact on western U.S in April-May (Zhang et al., 2008; Lin et al., 2015; Gratz et al., 2014). Based on the meteorological patterns that best facilitate long-range transport over the Pacific, such as more frequent cyclonic activity in the late spring (Liang et al., 2005), we similarly placed the emphasis only on April-May for the trajectory generation in spring. Trajectories were also computed for summer (June-August) because high O_3 events have been observed to associate with hot, sunny weather conditions over urban areas with high vehicle, residential and industrial emissions; consequently, elevated ground-level O_3 is primarily considered to be a

summertime problem (CDPHE, 2015). The analysis for summertime trajectories is used as a contrast to springtime to capture the peak in local photolysis and O_3 production.

The HYSPLIT Trajectory Cluster Analysis was applied to identify distinct transport patterns of O_3 and its precursors. Once the trajectories indicating the flow patterns have been computed, trajectories that are similar to one another in direction of advection and velocity of air movement can be grouped together into clusters (Stein et al., 2016). Each cluster only indicates a broad distribution suggesting potential transport pathway and altitude. Differences between trajectories within a cluster are minimized while differences between clusters are maximized (Stein et al., 2016). Grouping trajectories into clusters not only simplifies the analysis and interpretation, but also reduces the uncertainty in establishing the atmospheric transport pathways (Fleming et al., 2012; Stein et al., 2016). Therefore, the suggested clusters are useful for categorizing the distinct long-term transport patterns at the Manitou Springs station.

For springtime cluster analysis (April-May), trajectories starting every fourth hour beginning with 0:00 UTC (six trajectories per day) were used. For summertime cluster analysis (June-August), trajectories starting every eighth hour beginning with 4:00 UTC (three trajectories per day) were included. This difference in trajectory calculations between the two seasons is due to the memory limits of the program, unfortunately leaving half of the trajectories computed for summer unused. Every 12^{th} endpoint along the trajectory was used in both clustering procedures. In total, 3840 trajectories were included and eight distinct clusters were identified for spring; 3037 trajectories were included and nine distinct clusters were identified for summer. To combine the hourly O_3 measurements collected in the Manitou Springs station with the every-fourth-hour

(springtime) and every-eighth-hour (summertime) trajectories, the hourly measurements around the start time of trajectories were averaged. For example, for a trajectory beginning at 4:00 in spring, O_3 measurements from 2:00-5:00 were averaged; for a trajectory beginning at 4:00 in summer, O_3 measurements from 0:00-7:00 were averaged. It is worth mentioning that the starting times for summertime cluster analysis were 4:00, 12:00, and 20:00, in which two of the starting times were during the nighttime when photolytic activities were weak; thus 8 hour averaged O_3 values assigned to the clusters starting at 4:00 and 20:00 might be lower in general.

3. Results

3.1. Annual and seasonal O_3 trends

From 2005 to 2015, the annually averaged and 95th percentile O_3 data did not indicate significant linear trends, while the 5th percentile O_3 increased significantly by 0.82 ppbv yr^{-1} (5.77% yr^{-}, Fig. 3). There was a strong seasonal variability, in which the medians for spring (45 ppbv) and summer (46 ppbv) were significantly higher than the fall (36 ppbv) and winter (35 ppbv) (Fig. 4). Concentrations of O_3 and its precursors usually follow seasonal cycles, in part because of their strong dependence on solar radiation and the seasonal variations in day length and the angle of the sun (CDPHE, 2015).

For seasonal trends, there were no significant linear trends in spring- or summertime O_3. The 50th and 95th percentiles for spring (March-May), just April-May, and summertime O_3 showed decreasing tendencies, but trends were not significant (Fig. 4 and Table 1). The 5th percentile O_3 for both of the spring and summer had positive trends, but trends were also not significant (Fig. 4). The only significant trends were found in the

wintertime; the 5th and 50th percentiles wintertime O_3 increased significantly by 0.30 ppbv yr^{-1} in the 50th percentile (0.9% ppbv yr^{-1}) and 1.13 ppbv yr^{-1} in the 5th percentile (17.2% ppbv yr^{-1}), while the 95th percentile did not show a significant linear trend (Table 1). For fall O_3 trends, the 5th, 50th and 95th percentiles all showed increasing trends, but none were significant.

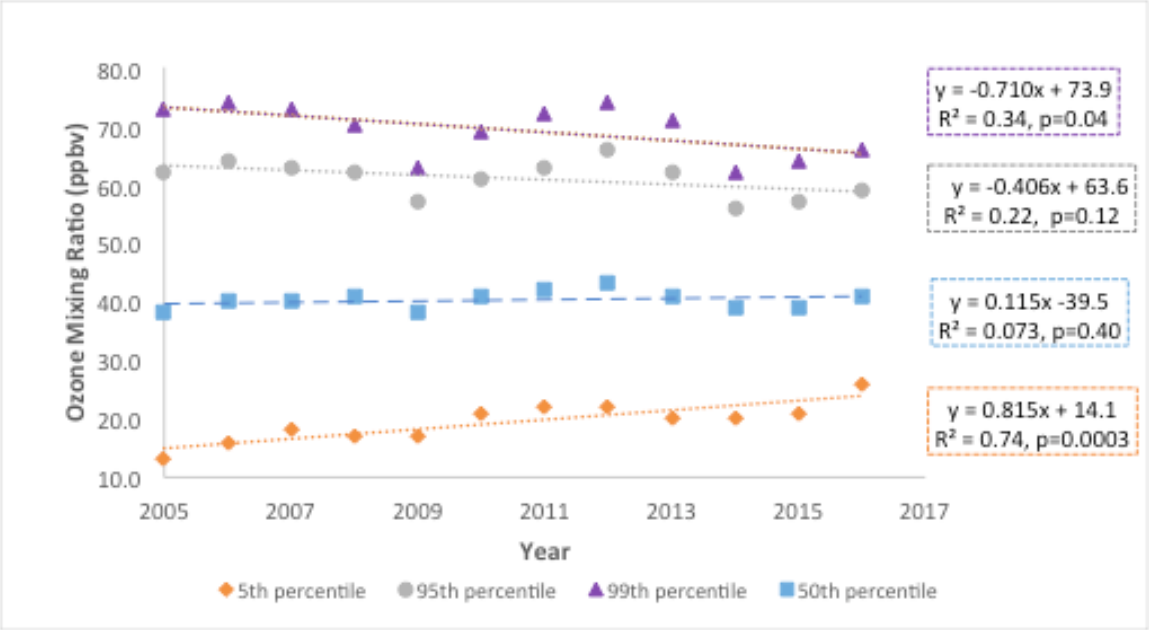

Figure 3 5th percentile (orange diamond), 50th percentile (blue square), 95th percentile (grey circle), and 99th percentile (purple triangle) annual O_3 mixing ratios at the Manitou Springs station from 2005 to 2015, with associated linear regressions.

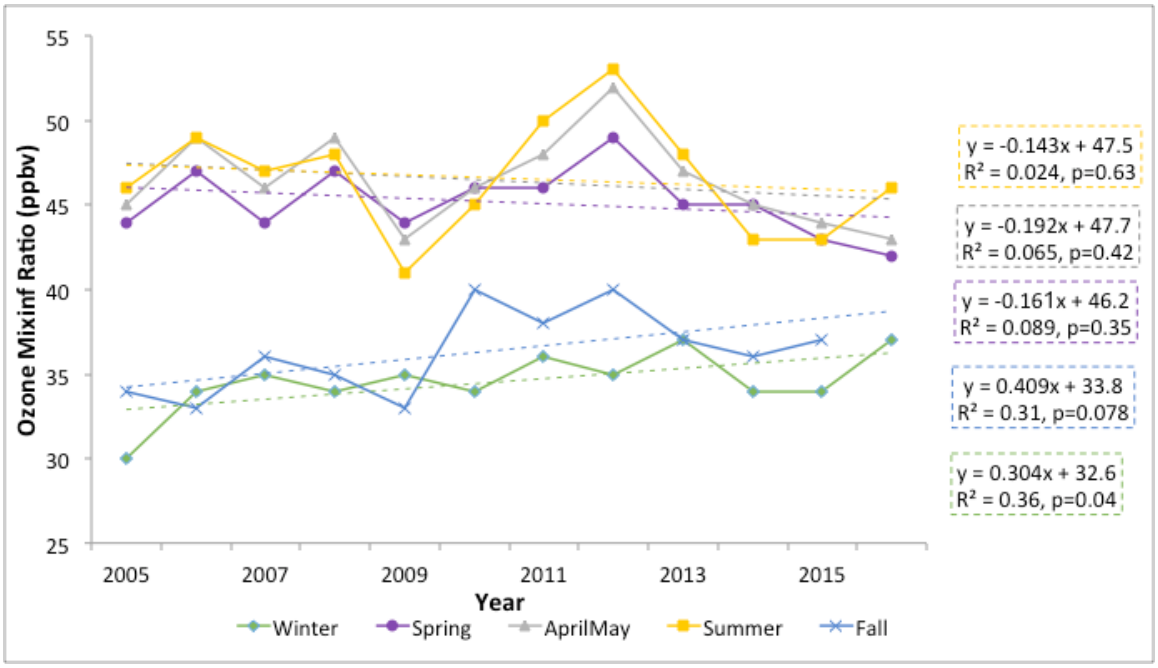

Figure 4 Seasonal trends from 2005 to 2016, with associated linear regressions.

3.2 HYSPLIT cluster analysis

3.2.1 Cluster characterization

Fig. 5 shows eight distinct back-trajectory paths and altitudes for springtime clusters. In most cases, a cluster includes hundreds of trajectories. Clusters 3 and 5 represent high-altitude trans-Pacific transport in the free troposphere from regions of East Asia, with Cluster 5 displaying the fastest and the longest transport all the way back to Europe (Fig. 5). Clusters 1 and 4 indicate transport across the North Pacific. Clusters 2 and 6 represent relatively slow and low-altitude transport over the Pacific. Clusters 4 and 5 have the highest 50th percentile O_3, and Clusters 7 have the lowest 50th percentile O_3 (Table 2). Cluster 5 has the fewest number of trajectories (n=36), with no trajectories assigned to it in 2006 and 2007.

Table 1 Linear regression statistics for O_3 within each season.

Ozone	5th percentile				50th percentile				95th percentile			
Season	m (ppbv/yr)	b (ppbv)	R^2	p	m (ppbv/yr)	b (ppbv)	R^2	p	m (ppbv/yr)	b (ppbv)	R^2	p
Spring	0.34	23.12	0.25	0.10	-0.16	46.21	0.09	0.35	-0.24	62.97	0.08	0.38
AprilMay	0.21	24.82	0.06	0.46	-0.19	47.67	0.07	0.42	-0.21	64.36	0.06	0.46
Summer	0.47	23.95	0.24	0.10	-0.14	47.52	0.02	0.63	-0.70	71.11	0.30	0.07
Fall	0.59	13.00	0.35	0.06	0.41	33.82	0.31	0.08	0.12	52.45	0.02	0.67
Winter	1.13	6.55	0.65	0.00	0.30	32.61	0.36	0.04	0.00	47.74	0.01	0.98

Table 2 5th, 50th and 95th percentiles for springtime O_3 within HYSPLIT Clusters 1-8.

Cluster	N	50th percentile	5th percentile	95th percentile
1	176	47.8	32.5	64.1
2	998	46.5	26.2	63.5
3	224	46.9	32.1	61.5
4	680	48.5	30.8	64.7
5	36	48.6	33.9	59.7
6	828	46.5	26.9	63.8
7	514	45.3	23.9	61.3
8	356	46.3	22.2	63.6

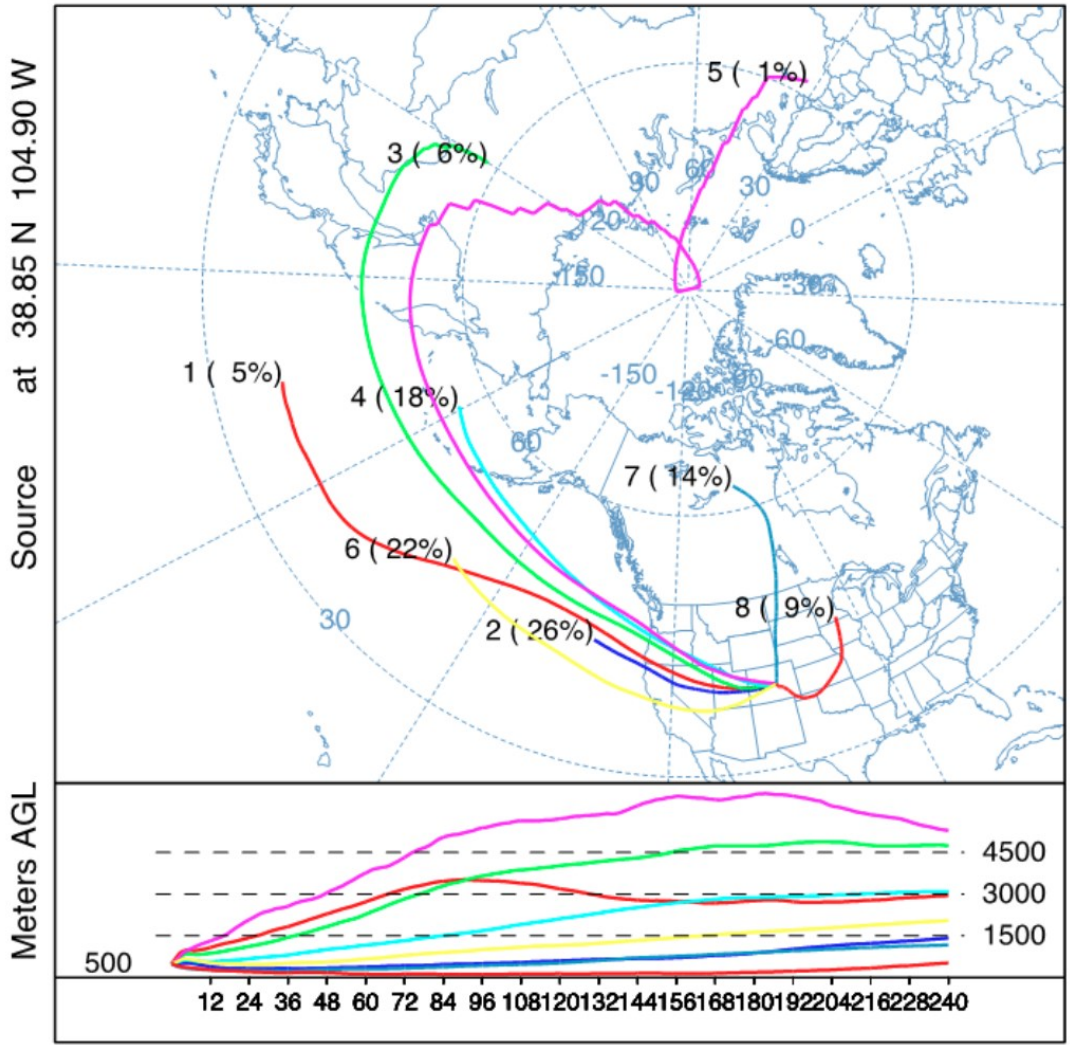

Figure 5 Springtime mean air mass back-trajectories and mean trajectory heights (m above ground level) for each HYSPLIT cluster.

Fig. 6 displays the mean back-trajectory paths and altitudes for summertime clusters. In total, nine cluster groups were computed. None of the clusters reached the continent of Asia. Clusters 3 and 5 represent high-altitude North Pacific transport in the free troposphere, with cluster 5 showing the fastest long-range transport. Clusters 1 and 4 represent relatively slow and low-altitude flow over the Pacific. Clusters 5 and 8 have the

highest 50th percentile O_3, and clusters 2 and 9 have the lowest 50th percentile O_3 (Table 3). Cluster 5, the longest and fastest transport, has the fewest number of trajectories (n=82). Moreover, for both spring and summer, no significant trends in the number of trajectories assigned to any clusters were found, suggesting that the frequency of transport did not have any influence over the O_3 trends observed at the Manitou Springs station.

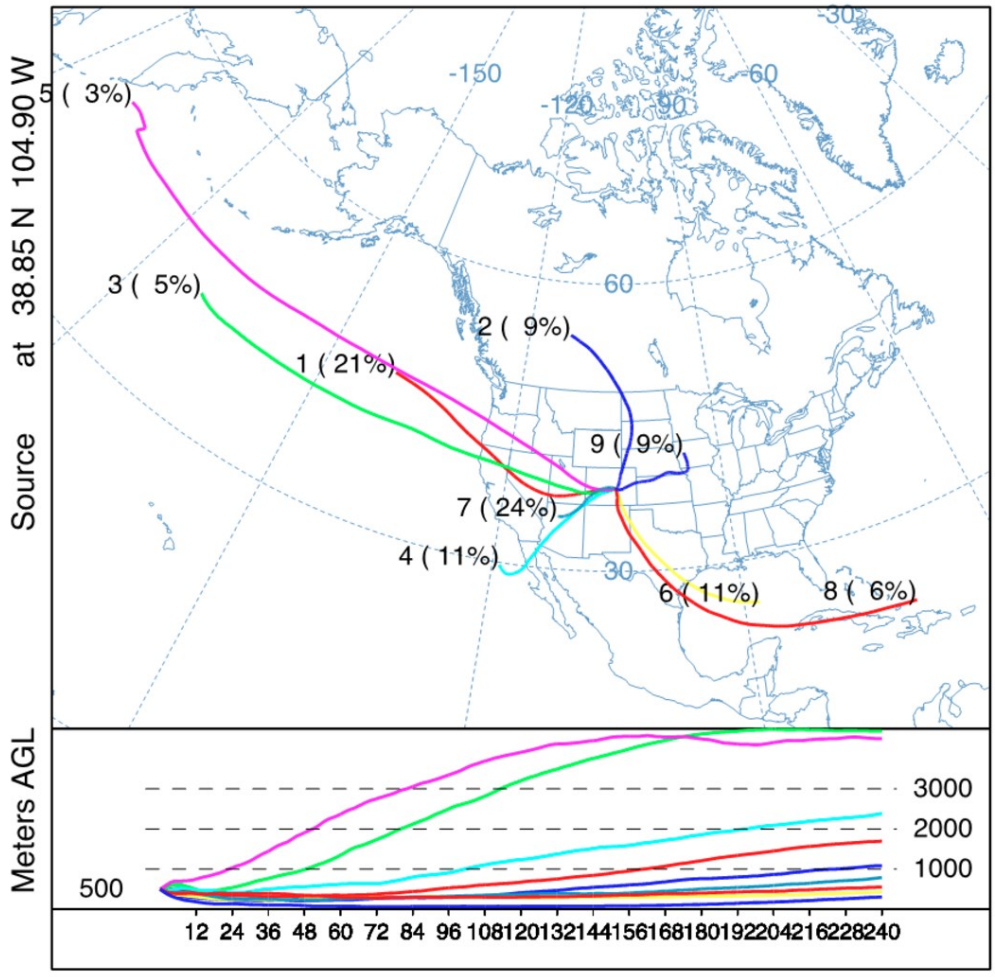

Figure 6 Summertime mean air mass back-trajectories and mean trajectory heights (m agl) for each HYSPLIT cluster.

Table 3 5th, 50th and 95th percentiles for summertime O_3 within HYSPLIT Clusters 1-9.

Cluster	N	5th percentile	50th percentile	95th percentile
1	626	29.5	47.5	64.3
2	276	24.5	45.0	66.4
3	146	31.0	48.6	63.7
4	331	30.3	44.3	61.8
5	82	32.6	46.3	68.6
6	338	29.4	49.1	64.1
7	728	30.0	47.2	65.6
8	193	33.2	48.1	64.4
9	281	23.6	44.8	64.1

3.2.2 O_3 trends within HYSPLIT clusters

Table 4 represents the springtime O_3 trends within clusters 1-8. Most clusters do not display significant linear trends. Only cluster 2 has a significant positive trend in the 5th percentile with an increase of 0.83 ppbv yr^{-1} (3.8% ppbv yr^{-1}; Table 4). Table 5 indicates the summertime O_3 trends within clusters 1-9. Cluster 2 has a significant decrease in the 95th percentile of 1.72 ppbv yr^{-1} (2.5% ppbv yr^{-1}; Table 5). Cluster 6 increases significantly in the 5th percentile by 1.21 ppbv yr^{-1} (5.3% ppbv yr^{-1}; Table 5).

Table 4 Linear regression statistic for springtime O_3 within HYSPLIT Clusters 1-8. Trends for Cluster 5 started from 2008, because of the lack of data in 2006 and 2007.

Ozone		5th percentile			50th percentile				95th percentile			
Cluster	m (ppbv/yr)	b (ppbv)	R^2	p	m (ppbv/yr)	b (ppbv)	R^2	p	m (ppbv/yr)	b (ppbv)	R^2	p
1	-0.46	33.96	0.06	0.465	-0.07	48.26	0.00	0.911	-0.28	59.38	0.02	0.681
2	0.83	22.15	0.49	0.016	0.15	44.56	0.02	0.718	-0.40	30.86	0.03	0.637
3	-0.28	48.24	0.04	0.555	-0.40	50.32	0.08	0.410	-0.25	29.95	0.07	0.420
4	-0.25	48.95	0.03	0.593	-0.27	49.53	0.08	0.388	-0.90	43.56	0.24	0.128
5	0.14	44.34	0.04	0.620	-0.03	46.75	0.00	0.980	0.71	45.36	0.12	0.286
6	0.00	27.35	0.05	0.490	-0.22	48.31	0.04	0.549	-0.43	67.58	0.06	0.456
7	0.57	21.69	0.14	0.259	0.19	43.17	0.04	0.552	0.16	61.62	0.01	0.745
8	0.05	26.37	0.00	0.951	-0.50	48.78	0.16	0.226	0.18	58.10	0.01	0.790

Table 5 Linear regression statistic for summertime O_3 within HYSPLIT Clusters 1-9.

□		5th percentile			50th percentile				95th percentile			
Cluster	m (ppbv/yr)	b (ppbv)	R^2	p	m (ppbv/yr)	b (ppbv)	R^2	p	m (ppbv/yr)	b (ppbv)	R^2	p
1	-0.05	29.55	0.00	0.929	-0.07	48.22	0.00	0.865	-0.39	65.79	0.05	0.519
2	-0.03	28.78	0.00	0.962	-0.46	48.75	0.12	0.307	-0.74	65.64	0.21	0.157
3	0.08	30.00	0.00	0.896	0.04	45.79	0.00	0.944	-0.34	61.20	0.03	0.604
4	0.00	30.75	0.00	0.998	-0.27	48.62	0.04	0.576	-0.59	65.55	0.22	0.143
5	0.36	32.39	0.03	0.625	-0.33	48.69	0.03	0.610	-1.72	69.34	0.37	0.049
6	1.21	22.82	0.42	0.032	0.37	46.64	0.13	0.269	-0.33	67.39	0.14	0.249
7	0.19	28.97	0.02	0.667	-0.04	47.75	0.00	0.940	-0.69	67.40	0.15	0.233
8	0.28	31.48	0.06	0.451	-0.53	50.89	0.13	0.280	-0.42	63.91	0.08	0.403
9	0.99	21.10	0.31	0.076	-0.09	46.99	0.01	0.806	-0.71	67.99	0.13	0.273

4. Discussion

4.1 Compliance with the lowered O_3 NAAQS

On October 1st, 2015, the U.S. EPA tightened the ground level O_3 standard to 0.070 ppm (70 ppbv) averaged over an 8-hour period (EPA, 2017). In this study, I did not follow EPA's designation guideline to analyze the O_3 data, because rather than only focus on standard violations, this study analyzed the full range of O_3 values, reporting trends in different percentiles. Nevertheless, from 2005 to 2016, none of the annual 95th percentile O_3 values exceeded the 70 ppbv threshold, and the annual trend analysis captured a decreasing trend in the annual 95th percentile O_3, but the trend was not significant. While some individual annual 99th percentile O_3 values exceeded 70 ppbv, the annual 99th percentile O_3 displayed a significant decrease with a slope of -0.71 ppbv yr^{-1} (-0.96% yr^{-1}, Fig 2). The annual 99th percentile O_3 values for 2015 and 2016 are 64 and 66 ppbv, respectively, well below the current standard, and the trend analysis suggests a decreasing tendency. Thus, according to the data collected at the Manitou Springs station, it appears unlikely that Colorado Springs would be designated as non-attainment under the lowered NAAQS for O_3.

4.2 Annual trends

As mentioned earlier, over the past decades, regulatory and emission controls have resulted in nationwide reductions in O_3 precursor emissions (EPA, 2016; Parrish et al., 2012). A number of studies have reported decreasing 95th percentile O_3 trends at several eastern U.S. sites, indicating the substantial decline in both frequency and magnitude of high O_3 pollution events, which also demonstrates the effectiveness of regional controls of O_3 precursor emissions (Parrish et al., 2012; Simon et al., 2014). The

annually averaged O_3 data at the Manitou Springs station also showed a decreasing tendency at the 95th percentile, but the trend was not significant (-0.64% ppbv yr^{-1}, p=0.12).

While the annual 95th percentile O_3 appeared to be decreasing, the annual 5th percentile had a significant increasing trend (5.77% ppbv yr^{-1}). Several studies also found that the mixing ratios of the lower O_3 percentiles, such as the 5th and 10th percentiles, were increasing at some rural sites in the western U.S., especially during spring, suggesting that the increase in the lower O_3 percentiles was due to an increase in baseline O_3 flowing into the U.S. from Asia (Cooper et al., 2012; Parrish et al., 2012; Simon et al., 2014). Moreover, according to Cooper et al. (2012), decreasing local NO_x emissions may also contribute to the rise in lower O_3 percentiles, as urban areas will experience less NO_x titration under weak photochemical conditions.

4.3 Seasonal trends

The O_3 seasonal cycle is strongly driven by seasonal changes in photochemistry and temperature. The observed surface O_3 seasonal cycle at the Manitou Springs station is also influenced by O_3 concentrations that have a varying mix of local, regional, and long-distance origins. The O_3 data at the Manitou Springs station shows a seasonal cycle with spring and summertime 50th percentile O_3 significantly higher than the fall and wintertime 50th percentile O_3. This indicates that although changes in the emissions of O_3 precursors can strongly influence surface O_3 concentrations, the seasonal variability may actually have a greater effect on surface O_3 concentrations than anthropogenic emissions. As O_3 is generated by photochemical reactions in the troposphere, the rate of some of the reactions increases with temperature and solar intensity, and O_3 production generally

reaches a maximum in sunny days with high temperatures (Sillman, 2003). High O_3 concentration events in the spring and summer may also be attributed to both enhanced stratospheric intrusions and the peak in local and regional photochemical production at this time of year (Parrish et al., 2013). Moreover, Asian pollution can be transported across the Pacific to the surface of western North America mostly by frontal lifting in WCBs, convection, and orographic lifting, and the transport is most rapid and frequent in spring due to active cyclonic activity and strong westerly winds (Zhang et al., 2008).

4.3.1 Springtime O_3 trends

For the springtime O_3 trends, although multiple studies have observed increases for springtime O_3 mixing ratio in the western US free troposphere (Cooper et al., 2012; Parrish et al., 2012; Zhang et al., 2008; Lin et al., 2017), no significant positive trends were found at any of the calculated percentiles in springtime O_3 observations at the Manitou Springs station from 2005 to 2016. Simon et al. (2014) evaluated O_3 trends at urban monitoring sites across the US from 1998 to 2013 and also found no statistically significant trends in springtime O_3 in several northwestern U.S. sites, explaining that substantial interannual meteorological variability may obscure longer-term trends due to emissions changes (Simon et al. 2014). Also, we acknowledge that a 12-year record is relatively short but still sufficient for trend analysis; however, the Manitou Springs station started operation in 2004, thus disallowing the examination of inter-decadal variability in tropospheric O_3 concentrations. Moreover, most of the previous O_3 trend studies were done at more remote or rural locations, such as national parks and the Mt. Bachelor Observatory, which are primarily influenced by transported regional or global emissions. In contrast, the Manitou Springs station may be more affected by the local

urban emissions from Colorado Springs and Denver than by the long-range transport of emissions, perhaps obscuring any impact of rising precursor emissions from outside the region or the US. Additionally, the Manitou Springs station is located at the base of Pikes Peak, which is on the eastern side of the Continental Divide, whereas many of the studies that have seen significant rising O_3 during spring are on the western side of the Continental Divide. Thus, the complex topography and meteorology at the Manitou Springs station might affect the local dominant transport patterns compared to other western study sites.

Although no significant trend for springtime O_3 was found in this research, previous studies have evaluated springtime O_3 trends, and a number of researchers have investigated trends in baseline O_3 concentrations at rural and remote sites. Recently, a study by Lin et al. (2017) examined changes in U.S. surface O_3 means and extremes from 1980 to 2014, and they found positive springtime trends at western U.S. rural sites with a 0.2-0.5 ppb yr^{-1} increase. They also acknowledge that the Asian NO_x emissions have tripled since 1990, contributing as much as 65% to modeled springtime background O_3 increases over the western U.S., counteracting O_3 decreases attained via O_3 precursor emission controls (Lin et al. 2017). This study included the USAFA as one of their observation sites for analysis, thus I also briefly looked at the USAFA O_3 data from 2005 to 2016. The annual 5^{th} and 50^{th} percentiles indicate significant positive trends with slopes of 0.8 ppbv yr^{-1} and 0.65 ppbv yr^{-1} (Fig 8), which is consistent with the general trends in the western US reported in Lin et al., (2017). On the other hand, none of the calculated percentiles springtime O_3 showed significant trends from 2005 to 2016; whereas Lin et al. (2017) found significant springtime O_3 increases occur at all observed

percentiles at the USAFA station. One possible explanation is that the time interval for trend analysis in my study (2005-2016) is much shorter than the time interval in Lin et al. (2017). This suggests that trends have been occurring at this site, but a 12-year dataset was not enough to identify significant trends. Similar trends might be detected, if O_3 measurements from 1996 to 2016 were analyzed. Moreover, the 5th percentile for summertime O_3 showed a significant positive trend of 0.73 ppbv yr^{-1} (24% ppbv yr^{-1}), which is consistent with trends reported by Lin et al., (2017).

For the springtime cluster analysis at Manitou Springs, most clusters do not show significant linear trends except the 5th percentile of Cluster 2 with an increase of 0.83 ppbv yr^{-1} (3.8% ppbv yr^{-1}). Cluster 2 represents relatively low-altitude flow over the Pacific, and it does not reach the continent of Asia (Figure 5); thus, Asian O_3 pollution cannot be confirmed as the cause of the increase in O_3 to according to the cluster analysis. However, as Asian O_3 pollution is transported across the Pacific, the time to reach the surface of western North America can be on the order of 2-3 weeks (Zhang et al., 2008). Since this research computed 10-day backward trajectories, the time interval may not be long enough to capture the trans-Pacific transport of O_3 for Cluster 2.

4.3.2 Summertime O_3 trends

Ozone is generally considered to be a summertime pollutant, and the "ozone season" in Colorado is defined from March to September (CDPHE, 2015). According to the O_3 data collected at the Manitou Springs station, the highest O_3 concentrations usually occur in summer months, which is consistent with this statement. High O_3 events tend to occur in response to high surface temperature, low wind speeds, clear skies, and stagnant conditions associated with strong subsidence inversions, which allow pollutants to

accumulate near the surface (Jacob, 1999; Shen & Mickley, 2017). In summer, the intensified radiation and higher temperatures facilitate the O_3 formation process and thus lead to high concentrations. For summertime trends, studies have reported decreases in the 95th percentile O_3 concentrations during the summer across the U.S. due to regional O_3 precursor emission controls (Clifton et al., 2014; Simon et al., 2015; Cooper et al., 2012). However, in the analysis of O_3 data at the Manitou Springs station, although the 50th and 95th percentiles for summertime O_3 decreased from 2005 to 2016, both were not significant (Table 1), suggesting less detectable trends in O_3 here compared to other studies (Cooper et al., 2012; Lin et al., 2017). Possible explanations are, similar to the springtime trends, the geographical location of the monitoring station and influence from local urban emissions.

For the summertime cluster analysis, the 95th percentile of Cluster 5 shows a significant decrease of 1.72 ppbv yr^{-1} (2.5% ppbv pr^{-1}). Cluster 5 represents high-altitude North Pacific transport in the free troposphere, and it is the fastest and longest transport within the summertime clusters. However, Cluster 5 did not reach the continent of Asia. Since regional O_3 concentrations reflect a varying mix of local, regional and long-distance origins, it is difficult to accurately determine air transport and mixing histories using back trajectories alone. I hypothesize that the reduction of O_3 precursor emissions on local scale may contribute to the decreases at the 95th percentile at the Manitou Springs station. On the other hand, the 5th percentile of Cluster 6 increased significantly by 1.2 ppbv yr^{-1} (5.3% ppbv yr^{-1}). Cluster 6 represents southeastern low-attitude transport from the Gulf of Mexico, and it also has the highest 50th percentile (49.1 ppbv) within the summertime clusters. Recent increases in NO_x and VOC emissions associated with the

production of oil and natural gas may contribute to this trend. A study done in the Colorado Northern Front Range found that oil and natural gas alkanes contribute approximately 20% to regional photochemical O_3 production (McDuffie et al., 2016). It is plausible that air arriving at the Manitou Springs station from the northeast may have traveled over regional oil and natural gas operations, carrying O_3 precursors with it.

4.3.3 Wintertime O_3 trends

Unexpectedly, the winter O_3 data at the Manitou Springs station indicates significant positive trends in the 50^{th} (0.93% ppbv yr^{-1}) and 5^{th} percentiles (17.2% ppbv yr^{-1}). This is, however, consistent with trends reported by a few recent studies across the country (Lin et al., 2017; Simon et al., 2014; Clifton et al., 2014, Cooper et al., 2012). For example, Simon et al. (2014) found that 5^{th} percentile O_3 generally increased by 0.1-1 ppbv yr^{-1} in winter from 1998-2003, and also reported that positive O_3 trends generally occur in more urbanized areas and at the lower O_3 percentiles. Studies observed that across-the-board NO_x decreases might result in widespread increases in wintertime O_3 because of the influence from weakened NO_x titration (Lin et al., 2017; Cooper et al., 2012). Moreover, emerging science is indicating that snow-covered oil and gas-producing basins in the western U.S. are at the risks of exceeding the NAQQS for O_3 in winter, because sunlight reflected off snow-covered surfaces can enhance the photochemistry that increases O_3 formation (CPDHE, 2015). Similar effects were observed by a few recent studies such as one in the Upper Green River Basin in Wyoming (Edward et al., 2014). The Upper Green River Basin has experienced rapid development of the oil and natural gas industry over the last several years. Oil and natural gas extraction stations are operating continuously and emitting significant amount of NO_x and VOCs. A study

reported that the oil and natural gas extraction was the only significant emission source in the Upper Green River Basin area with overall emissions of 9.9 t day^{-1} of reactive NO_x and 41.7 t day^{-1} of VOCs, respectively, resulting exceptionally high O_3 concentrations in the wintertime. (Rappenglück et al., 2014). Moreover, studies also found that oil and natural gas operations contribute significant amounts of methane as well as non-methane hydrocarbons, such as ethane and propane, to the atmosphere (Ahmadov et al., 2015). Previous studies indicate that high O_3 episodes were associated with below-freezing temperatures, persistent snow cover, and prevailing light wind conditions (Ahmadov et al., 2015). Such stable atmospheric conditions could produce strong, shallow temperature inversions that trap fossil fuel emissions in a stable boundary layer allowing for a build-up of O_3 precursor chemicals (Edwards et al., 2014). Sunlight passing through the trapped pollutants and reflecting back of the high albedo snow cover can increase the rate of photochemical production of O_3 during the day (Ahmadov et al., 2015). This may explain the significant increase in wintertime O_3 in Manitou Springs, which may be influenced by transport of O_3 and its precursors along the Front Range.

5. Conclusion

I have analyzed the hourly O_3 measurements at the Manitou Springs station from 2005 to 2016 to determine long-term trends. Overall, decreasing trends were generally found at the upper percentiles across the trend analysis; however most of them were not statistically significant. The decreases in high O_3 concentrations may attribute to the effectiveness of both local and nationwide O_3 precursor emission controls. The 5^{th} percentiles generally showed increasing trends, indicating possible increased baseline ozone; however only the trend in the 5^{th} percentile in wintertime O_3 was significant. I

hypothesize that the lack of significant trends is possibly due to the geographical location of the monitoring station and influence of local urban emissions. The 50th percentile had a more mixed result. The 50th percentiles for annual, spring, and summer showed decreasing tendencies, but not they were significant, whereas wintertime O_3 significantly increased in the 50th percentile. Rapid development of the oil and natural gas industry around the region may contribute to the rising trends in the wintertime O_3. I also performed cluster analysis of 10-day HYSPLIT back-trajectories for spring (April-May) and summer (June-August) months. For springtime, only Cluster 2, representing the low-altitude transport over the Pacific, had a significant positive trend in the 5th percentile. For the summertime cluster analysis, a significant positive trend in the 95th percentile was found in Cluster 6, the cluster is associated with the slow low-attitude transport from the southeast. For future research, to better examine baseline conditions at the Manitou Springs station, the O_3 data need to be filtered to remove the influence from local emission. Lin et al. (2017) used a set of regional CO-like tracers to filter out O_3 measurements based on the dominant influence of different continental air regimes, and this method can be implemented in future research. Moreover, this study did not evaluate the influence from stratospheric intrusions on spring and summer time O_3, because we did not have the data showing when exactly intrusion events happened, thus I wasn't able to conclude which high O_3 events were impacted by stratospheric intrusions. It would be worthwhile to consider the impact of stratospheric intrusions on the annual variability of high O_3 events in further research. Moreover, future studies should also incorporate data for the local O_3 precursors (i.e. NO_x, VOCs, and CO), which are not measured at the Manitou Springs station, to determine the local influence on the changes in O_3

concentrations. Lastly, only spring and summer time trajectories were generated in this study, because these are the seasons that are most likely to exceed the NAAQS for O_3; however, increasing trends were observed in winter, thus, future research should also run trajectory analysis for winter to look at local and regional source impacts, such as the impacts of oil and natural gas industry.

References:

Ahmadov, R., Mckeen, S., Trainer, M., Banta, R., Brewer, A., Brown, S., Edwards, P.M., Gouw, J.A.D., Frost, G.J., Gilman, J., Helmig, D., Johnson, B., Karion, A., Koss, A., Langford, A., Lerner, B., Olson, J., Oltmans, S., Peischl, J., Pétron, G., Pichugina, Y., Roberts, J.M., Ryerson, T., Schnell, R., Senff, C., Sweeney, C., Thompson, C., Veres, P., Warneke, C., Wild, R., Williams, E.J., Yuan, B., & Zamora, R. 2015. Understanding high wintertime ozone pollution events in an oil and natural gas producing region of the western US.*Atmospheric Chemistry and Physics Discussions*. 14(14):20295–20343.

Austin, E., Zanobetti, A., Coull, B., Schwartz J., Gold DR., Koutrakis., P., 2014. Ozone trends and their relationship to characteristic weather patterns. *Journal of Exposure Science and Environmental Epidemiology*, 25(5), pp.532–542.

Baylon, P.M., Jaffe, D.A., Pierce, R.B., & Gustin, M.S. 2016. Interannual Variability in Baseline Ozone and Its Relationship to Surface Ozone in the Western U.S.*Environmental Science & Technology*. 50(6):2994–3001.

Carter, W.P. & Seinfeld, J.H., 2012. Winter ozone formation and VOC incremental reactivities in the Upper Green River Basin of Wyoming. *Atmospheric Environment*, 50, pp.255–266.

CDPHE, 2013. EPA lowers federal ozone standard; Colorado, other states face more difficult compliance. *EPA lowers federal ozone standard; Colorado, other states face more difficult compliance | Department of Public Health and Environment*. Available at: https://www.colorado.gov/pacific/cdphe/news/ozone [Accessed April 18, 2017].

CDPHE, 2016. 2015 Air Quality Data Report. *Colorado Air Pollution Control Division*. Available at: http://www.colorado.gov/airquality/tech_doc_repository.aspx?action=open&file=2015AnnualDataReport.pdf

CDPHE, 2016. Colorado Annual Monitoring Network Plan 2016. *Colorado Air Pollution Control Division Technical Services Program*. Available at: http://www.colorado.gov/airquality/tech_doc_repository.aspx?action=open&file=2016AnnualNetworkPlan.pdf [Accessed April 18, 2017].

CDPHE., 2017 Technical Documents & Reports. *CDPHE - Colorado.gov/AirQuality*. Available at: http://www.colorado.gov/airquality/tech_doc_repository.aspx [Accessed April 18, 2017].

Clifton, O.E., Fiore, A.M., Correa, G., Horowitz, L.W., & Naik, V. 2014. Twenty-first century reversal of the surface ozone seasonal cycle over the northeastern United States. *Geophysical Research Letters*. 41(20):7343–7350.

Colorado Department of Tourism, Colorado Springs. Available at: http://www-scf.usc.edu/~csgustaf/itp104/project/colorado_springs.html [Accessed April 18, 2017].

Colorado Parks, Recreation, Trails, Open Space & Cultural Services, 2014. *City of Colorado Springs Park System Master Plan*, Colorado Springs, CO: City of Colorado Springs Parks, Recreation & Cultural Services .

Cooper, O.R., Parrish, D.D., Stohl, A., Trainer, M., Nédélec, P., Thouret, V., Cammas, J.P., Oltmans, S.J., Johnson, B.J., Tarasick, D., Leblanc, T., Mcdermid, I.S., Jaffe, D., Gao, R., Stith, J., Ryerson, T., Aikin, K., Campos, T., Weinheimer, A., & Avery, M.A. 2010. Increasing springtime ozone mixing ratios in the free troposphere over western North America. *Nature*. 463(7279): 344–348. Available at: http://www.nature.com/nature/journal/v463/n7279/full/nature08708.html.

Cooper, O.R., Gao, R.-S., Tarasick, D., Leblanc, T., & Sweeney, C. 2012. Long-term ozone trends at rural ozone monitoring sites across the United States, 1990-2010.*Journal of Geophysical Research: Atmospheres*. 117(D22).

Dawes, S.S., Burke, G.B. & Alteri, A., 2013. Air Quality Data Use, Issues, and Value in Colorado. Available at: https://www.ctg.albany.edu/publications/reports/sti_denver/sti_denver.pdf.

Draxler, R.R. & Hess, G.D., 1998. An Overview of the HYSPLIT_4 Modelling System for Trajectories, Dispersion, and Deposition. *Australian Meteorological Magazine*, 47(295). Available at: http://www.arl.noaa.gov/documents/reports/MetMag.pdf.

Edwards, P.M., Brown, S.S., Roberts, J.M., Ahmadov. R., Banta, R.M., deGouw, J.A., Dube, W.P., Field, R.A., Flynn, J.H., Gilman, J.B., Graus., M., Helmig, G., Koss, A., Langford, A.O., Lefer,B.L., Lerner, B.M., Li, R., Li, S., McKeen, S.A., Murphy, S.S., Parrish, D.D., Senffl, C.J., Soltis, J., Stutz, J., Sweeney, C., Thompson, C.R., Trainer, M.K., Tsai, C., Veres, P.R., Washenfelder, R.A., Warneke, C., Wild, R.J., Young, C.J., Yuan, B. & Zamora, R., 2014. High winter ozone pollution from carbonyl photolysis in an oil and gas basin. *Nature*, 514, pp.351–354. Available at: http://www.nature.com/nature/journal/v514/n7522/full/nature13767.html.

EPA, 2016. Air Quality Design Values. *EPA*. Available at: https://www.epa.gov/air-trends/air-quality-design-values [Accessed April 18, 2017].

EPA, 2017. Air Quality - National Summary. *EPA*. Available at: https://www.epa.gov/air-trends/air-quality-national-summary [Accessed April 18, 2017].

EPA, 2017. Ozone Basics. *EPA*. Available at: https://www.epa.gov/ozone-pollution/ozone-basics [Accessed April 18, 2017].

EPA, 2017. Ozone Designations Guidance and Data. *EPA*. Available at: https://www.epa.gov/ozone-designations/ozone-designations-guidance-and-data [Accessed April 18, 2017].

EPA, 2017. Table of Historical Ozone National Ambient Air Quality Standards (NAAQS). *EPA*. Available at: https://www.epa.gov/ozone-pollution/table-historical-ozone-national-ambient-air-quality-standards-naaqs [Accessed April 18, 2017].

Fleming, Z.C.A.B.L., Monks, P.S. & Manning, A.J., 2012. Review: Untangling the influence of air-mass history in interpreting observed atmospheric composition. *Atmospheric Research*, 104-105, pp.1–39. Available at: http://www.sciencedirect.com/science/article/pii/S0169809511002948?np=y&npKey=e0b6a55e824bf9ca7094157798982c14c10837c39ed9adbc8a94d7b36289615d.

Finlayson-Pitts, B. & Pitts, J., 1993. Atmospheric Chemistry of Tropospheric Ozone Formation: Scientific and Regulatory Implications. *Air & Waste*, 43(8), pp.1091–1100.

Gratz, L., Jaffe, D. & Hee, J., 2014. Causes of increasing ozone and decreasing carbon monoxide in springtime at the Mt. Bachelor Observatory from 2004 to 2013. *Atmospheric Environment*, 109, pp.323–330.

Jacob, D.J., 1999. *Introduction to Atmospheric Chemistry*, Princeton University Press. Ch11.

Liang, Q., Jaeglé, L., & Wallace, J.M. 2005. Meteorological indices for Asian outflow and transpacific transport on daily to interannual timescales.*Journal of Geophysical Research*. 110(D18).

Lin, M., Fiore, A.M., Horowitz, L.W., Cooper, O.R., Naik, V., Holloway, J., Johnson, B.J., Middlebrook, A.M., Oltmans, S.J., Pollack, I.B., Ryerson, T.B., Warner, J.X., Wiedinmyer, C., Wilson, J., & Wyman, B. 2012. Transport of Asian ozone pollution into surface air over the western United States in spring.*Journal of Geophysical Research: Atmospheres*. 117(D21).

Lin, M., Horowitz, L.W., Cooper, O.R., Tarasick, D., Conley, S., Iraci, L.T., Johnson, B., Leblanc, T., Petropavlovskikh, I., & Yates, E.L. 2015. Revisiting the evidence of increasing springtime ozone mixing ratios in the free troposphere over western North America.*Geophysical Research Letters*. 42(20):8719–8728.

Lin, M., Fiore, A.M., Horowitz, L.W., Langford, A.O., Oltmans, S.J., Tarasick, D., & Rieder, H.E. 2015. Climate variability modulates western US ozone air quality in spring via deep stratospheric intrusions.*Nature Communications*. 6:7105.

Lin, M., Horowitz, L.W., Payton, R., Fiore, A.M., & Tonnesen, G. 2017. US surface ozone trends and extremes from 1980 to 2014: quantifying the roles of rising Asian emissions, domestic controls, wildfires, and climate.*Atmospheric Chemistry and Physics*. 17(4):2943–2970.

Mcduffie, E.E., Edwards, P.M., Gilman, J.B., Lerner, B.M., Dubé, W.P., Trainer, M., Wolfe, D.E., Angevine, W.M., Degouw, J., Williams, E.J., Tevlin, A.G., Murphy, J.G., Fischer, E.V., Mckeen, S., Ryerson, T.B., Peischl, J., Holloway, J.S., Aikin, K., Langford, A.O., Senff, C.J., Alvarez, R.J., Hall, S.R., Ullmann, K., Lantz, K.O., & Brown, S.S. 2016. Influence of oil and gas emissions on summertime ozone in the Colorado Northern Front Range.*Journal of Geophysical Research: Atmospheres*. 121(14):8712–8729.

NASA., 2014. NASA Images Highlight U.S. Air Quality Improvement – Release Materials. *NASA*. Available at: https://svs.gsfc.nasa.gov/11579 [Accessed April 18, 2017].

Parrish, D.D., Law, K.S., Staehelin, J., Derwent, R., Cooper, O.R., Tanimoto, H., Volz-Thomas, A., Gilge, S., Scheel, H.-E., Steinbacher, M., & Chan, E. 2012. Long-term changes in lower tropospheric baseline ozone concentrations at northern mid-latitudes.*Atmospheric Chemistry and Physics Discussions*. 12(6):13881–13931. Available at: http://www.atmos-chem-phys.net/12/11485/2012/acp-12-11485-2012.pdf.

Parrish, D.D., Law, K.S., Staehelin, J., Derwent, R., Cooper, O.R., Tanimoto, H., Volz-Thomas, A., Gilge, S., Scheel, H.-E., Steinbacher, M., & Chan, E. 2013. Lower tropospheric ozone at northern midlatitudes: Changing seasonal cycle.*Geophysical Research Letters*. 40(8):1631–1636.

Rappenglück, B., Ackermann, L., Alvarez, S., Golovko, J., Buhr, M., Field, R.A., Soltis, J., Montague, D.C., Hauze, B., Adamson, S., Risch, D., Wilkerson, G., Bush, D., Stoeckenius, T., & Keslar, C. 2014. Strong wintertime ozone events in the Upper Green River basin, Wyoming.*Atmospheric Chemistry and Physics*. 14(10):4909–4934. Available at: http://www.atmos-chem-phys.net/14/4909/2014/acp-14-4909-2014.pdf.

Shen, L. & Mickley, L.J., 2017. Seasonal prediction of US summertime ozone using statistical analysis of large scale climate patterns. *Proceedings of the National Academy of Sciences*, 114(10), pp.2491–2496.

Sillman, S., 2003. Overview: Tropospheric ozone, smog and ozone-NOx-VOC sensitivity. *Ozone-NOx-VOC sensitivity*. Available at: http://www-personal.umich.edu/~sillman/ozone.htm [Accessed April 18, 2017].

Simon, H., Reff, A., Wells, B., Xing, J., & Frank, N. 2015. Ozone Trends Across the United States over a Period of Decreasing NOx and VOC Emissions.*Environmental Science & Technology*. 49(1):186–195. Available at: http://pubs.acs.org/doi/full/10.1021/es504514z.

Stein, A.F., Draxler, R.R., Rolph, G.D., Stunder, B.J.B., Cohen, M.D., & Ngan, F. 2015. NOAA's HYSPLIT Atmospheric Transport and Dispersion Modeling System.*Bulletin of the American Meteorological Society*. 96(12):2059–2077. Available at: http://journals.ametsoc.org/doi/full/10.1175/BAMS-D-14-00110.1.

Stohl, A., 1998. Computation, accuracy and applications of trajectories—A review and bibliography. *Atmospheric Environment*, 32(6), pp.947–966.

Strode, S.A., Rodriguez, J.M., Logan, J.A., Cooper, O.R., Witte, J.C., Lamsal, L.N., Damon, M., Aartsen, B.V., Steenrod, S.D., & Strahan, S.E. 2015. Trends and variability in surface ozone over the United States.*Journal of Geophysical Research: Atmospheres*. 120(17):9020–9042.

Sullivan, J.T., Mcgee, T.J., Thompson, A.M., Pierce, R.B., Sumnicht, G.K., Twigg, L.W., Eloranta, E., & Hoff, R.M. 2015. Characterizing the lifetime and occurrence of stratospheric-tropospheric exchange events in the rocky mountain region using high-resolution ozone measurements.*Journal of Geophysical Research: Atmospheres*. 120(24):12410–12424.

U.S. Chamber of Commerce, 2016. Ozone National Ambient Air Quality Standards. *U.S. Chamber of Commerce*. Available at: https://www.uschamber.com/issue-brief/ozone-national-ambient-air-quality-standards [Accessed April 18, 2017].

US Census Burean. Colorado Springs 2015 Population Estimate. *US Census Bureau*. Available at: https://www.census.gov/search-results.html?q=colorado%2Bsprings%2Bpopulation&search.x=0&search.y=0&search=submit&page=1&stateGeo=none&searchtype=web&cssp=SERP [Accessed April 18, 2017].

Weinhold, B., 2008. Ozone Nation: EPA Standard Panned by the People. *Environmental Health Perspectives*, 116(7). Available at: https://www.ncbi.nlm.nih.gov/pmc/articles/PMC2453178/.

Zhang, L., Jacob, D.J., Boersma, K.F., Jaffe, D.A., Olson, J.R., Bowman, K.W., Worden, J.R., Thompson, A.M., Avery, M.A., Cohen, R.C., Dibb, J.E., Flocke, F.M., Fuelberg, H.E., Huey, L.G., Mcmillan, W.W., Singh, H.B., & Weinheimer, A.J. 2008. Transpacific transport of ozone pollution and the effect of recent Asian emission increases on air quality in North America: an integrated analysis using satellite, aircraft, ozonesonde, and surface observations.*Atmospheric Chemistry and Physics Discussions*. 8(2):8143–8191.

Zhang, L., Jacob, D.J., Yue, X., Downey, N.V., Wood, D.A., & Blewitt, D. 2014. Sources contributing to background surface ozone in the US Intermountain West.*Atmospheric Chemistry and Physics*. 14(11):5295–5309.